Numerical simulation of nuclide transport at the underground repository scale subjected to thermal loading

Jintong Zhang
Tsinghua University, Beijing, China

Zhihong Zhao
Tsinghua University, Beijing, China

Junyu Chen
Tsinghua University, Beijing, China

Xingguang Zhao
Beijing Research Institute of Uranium Geology, Beijing, China

Ju Wang
Beijing Research Institute of Uranium Geology, Beijing, China

ABSTRACT: The nuclide transport with groundwater in the fractured rock is always the primary concern during the long-term operational life of underground repositories. The present paper intends to clarify the effects of thermal loading on in-situ stress, groundwater flow and solute transport at the repository scale. A three-dimensional repository model is built up incorporating a vertical fault and a horizontal fracture. The evolution of temperature, stress, aperture, flow velocity and nuclide transport at different time scales is analyzed and discussed. The thermal disturbance induces a significant distribution of temperature and contributes to the increased stresses in the rock matrix. The fracture and fault dominated convection and hydrodynamic dispersion are disturbed by the reduced aperture and the slow flow velocity around the repository. The nuclide transport is retarded under thermal loading conditions. The higher thermal conductivity in the repository induces to faster thermal decay and ultimately facilitates the nuclide transport.

Keywords: Nuclear waste repository, Nuclide transport, Thermal loading, Fracture, Thermal conductivity.

1 INTRODUCTION

Modelling the behavior of rock masses around repositories is of significance for the safety assessments of deep geological storage of nuclear waste because it requires predicting the retention of the repository for hundreds or even thousands of years (Guo et al. 2020; Chang et al. 2021). In addition, predicting nuclide transport behavior is necessary due to the need to ensure the long-term isolation of radioactive materials from the biosphere (Hudson et al. 2005; Chang et al. 2022). However, the heat release from the radioactive waste and spent nuclear fuel will generate heat waves that may disturb the stability of the repository system (Tsang et al. 2015).

The heat production from the radioactive waste induces the evolution of the temperature distribution around the repository. The thermal conductivity of the rock matrix and fractures control heat transport, and the density and heat capacity of the rock mass affect the heat transfer behavior during long-term operation. The thermal gradient influences the flow behavior by determining the viscosity and flow properties of water. Simultaneously, the hydraulic process affects the nuclide transport from the repository to the ground surface. In addition, the thermal expansion influences the deformability of rocks and fractures through matrix deformation and the aperture closure.

The main aim of this study is to develop a modeling framework on nuclide transport around a nuclear waste repository under thermal conditions. A 3D repository model including a vertical fault and a horizontal fracture was built up based on the validated 2D repository model in Min et al. (2005). The thermal effect on the nuclide transport was investigated incorporating the developed 3D model. In addition, the thermally induced temperature distribution, the interactions effects between heat and hydraulic, and the thermally induced mechanical behavior are taken into account.

2 METHODOLOGY

Here, the main governing equations are presented for describing the heat transfer and nuclide transport in fractures and matrices. The thermal and nuclide transport processes from emplacement of nuclear waste to long-term storage are provided in the developed model.

2.1 Modeling method

2.1.1 Thermal process

The heat transport in the fracture and the rock matrix is described by the conduction equation.

$$\rho_w C_w \left(v\frac{\partial T_f}{\partial y}+\frac{\partial T_f}{\partial t}\right)-\lambda_{fx}\frac{\partial^2 T_f}{\partial x^2}-\lambda_{fy}\frac{\partial^2 T_f}{\partial y^2}-\frac{\lambda_m}{b}\left(\frac{\partial T_m}{\partial z}\right)=0 \quad (1)$$

$$\frac{\partial T_m}{\partial t}-\frac{\lambda_{mx}}{C_m\rho_m}\frac{\partial^2 T_m}{\partial x^2}-\frac{\lambda_{my}}{C_m\rho_m}\frac{\partial^2 T_m}{\partial y^2}-\frac{\lambda_{mz}}{C_m\rho_m}\frac{\partial^2 T_m}{\partial z^2}=0 \quad (2)$$

where ρ_w is the density of the fluid, C_w is the heat capacity of fluid, T_f is the temperature in the fracture, λ_{fx} , λ_{fy} are the thermal dispersion coefficients in the directions of transverse and longitudinal in the fracture. T_m is the temperature in the rock matrix. λ_m is the mechanical dispersion coefficient associated with the concentration in the matrix. C_m is the heat capacity of the rock matrix, ρ_m is the density of the rock matrix, λ_{mx}, λ_{my} and λ_{mz} are the thermal conductivity in the directions of longitudinal, transverse horizontal, and transverse vertical, respectively.

2.1.2 Nuclide transport

The nuclide transport processes in the fracture are described by the conservative solute transport equations based on mass balance (Tang et al. 1981). The rock matrix is assumed impermeable to fluid flow due to its extremely low porosity. The nuclide is transported by diffusion in the porous matrix.

$$\frac{\partial c_f}{\partial t}+v\frac{\partial c_f}{\partial y}-D_{fx}\frac{\partial^2 c_f}{\partial x^2}-D_{fy}\frac{\partial^2 c_f}{\partial y^2}-\frac{D_m}{b}\frac{\partial c_m}{\partial z}=0 \quad (3)$$

$$\frac{\partial c_m}{\partial t}-D'_{fx}\frac{\partial^2 c_m}{\partial x^2}-D'_{fy}\frac{\partial^2 c_m}{\partial y^2}-D'_{fz}\frac{\partial^2 c_m}{\partial z^2}=0 \quad (4)$$

where c_f is the concentration of solute in the fracture, *t* is the time, *v* is the velocity of the fluid in the fracture, *x, y,* and *z* coordinates are the transverse direction in the fracture plane, the longitudinal direction in the fracture plane, and the vertical direction perpendicular to the fracture plane, respectively, c_m is the concentrations of solute in the rock matrix, b is the fracture aperture. D_m is the mechanical dispersion coefficient. The hydrodynamic dispersion coefficients D_{fx}, D_{fy} are defined associated with the molecular diffusion coefficient D^*. The coefficients D'_{fx}, D'_{fy} and D'_{fz} are the solute diffusion coefficients in the x, y and z directions of the matrix, respectively. Note that the other transport mechanisms such as sorption and decay are not considered for simplicity in this study.

$$D_{fx} = \alpha_x v + D^* \tag{5}$$

$$D_{fy} = \alpha_y v + D^* \tag{6}$$

where α_x, α_y are the transverse and longitudinal dispersity.

2.2 Model setup

A three-dimensional (3D) repository model is constructed in a cubic domain with side length of 1 km. The nuclear wastes are assumed to be emplaced into the repository of 10 m in height, 100 m in width, and 100 m in length (Fig. 1 (a)). A function (Eq. (7)) is taken to delineate the heat evolution after the emplacement of the waste canisters (Min et al., 2005). The vertical and horizontal in-situ stresses are linear depth-dependent following Eq. (8).

$$\begin{aligned} flux &= 1000, t \le 10, t = year \\ flux &= 10^{(-0.3979\log_{10} t + 3.3979)}, t \ge 10 \end{aligned} \tag{7}$$

$$\begin{aligned} \sigma_v &= -0.0252062D \\ \sigma_h &= -0.0331747D \end{aligned} \tag{8}$$

The inlet boundary (i.e., constant head) conditions are implemented at the bottom and the right boundaries. The outlet boundary conditions are applied at the top and the left boundaries (Fig.1 (b)). Table 1 shows the numerical parameters of the repository model. No flow conditions are imposed in other boundaries. The temperature at the top boundary is 11 °C, a constant basal heat flux of 54 mW/m^2 at the bottom boundary, and the geothermal gradient is 2.4 (°C/100 m). The lateral boundaries of the model are no-heat flow boundaries.

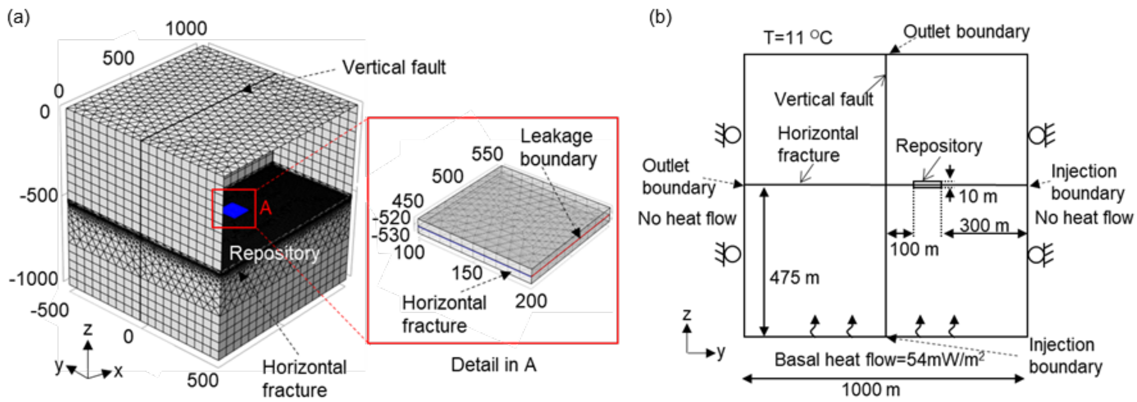

Figure 1. A 3D far-field repository model. (a) Mesh of model. (b) Boundary conditions.

Table 1. Numerical parameters of the nuclear waste repository.

Property	Symbol	Unit	Material	Value
Density	ρ_s	Kg/m^3	Matrix	2.52e+3
			Repository	1.60e+3
	ρ_w		Water	1.00e+3
Poisson's ratio	v	-	Matrix Repository	0.45
Young's modulus	E_i	GPa	Matrix Repository	17.69
Coefficient of thermal expansion	α_s	$\mu\varepsilon/K$	Matrix Repository	10
	α_w		Water	280
Heat capacity	C_m	J/kg/K	Matrix	0.80e+3
			Repository	0.87e+3
	C_w		Water	4.20e+3
Thermal conductivity	λ_s	W/mK	Matrix	2.30
			Repository	1.30
	λ_w		Water	0.65

3 RESULTS

The developed model is applied to investigate the thermally induced temperature, thermally induced stress and nuclide transport in the fractures. In addition, the varies thermal conductivities are taken into account to understand the thermal effect.

3.1 Temperature and stress

The evolutions of temperature and stress from 10^2 years to 10^5 years are demonstrated to validate the present model with the previous study (Min et al. 2005). Figure 2 shows the temperature and stress evolution on the vertical reference line (VRL) at the time scales of 10^2, 10^3, 10^4, and 10^5 years. Good agreement is observed between the previous far-field analysis (Min et al., 2005) and the present numerical simulation. The repository reaches the highest temperature (50.0 °C) after 10^2 years of emplacing spent fuel. Then, the temperature decreases with the heat decay until 10^5 years. Corresponding to the vary temperature, the thermally induces stress also rises to the maximum value at 10^2 years and gradually disappears until 10^5 years.

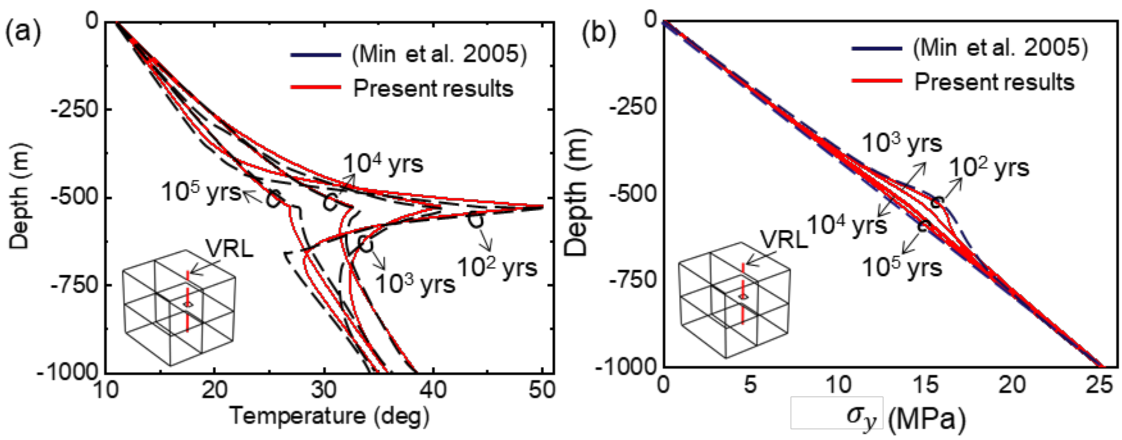

Figure 2. Evolutions of temperature and stress on the vertical reference line (VRL) at the time scales of 10^2, 10^3, 10^4, and 10^5 years. (a) temperature evolution and (b) stress evolution.

3.2 Nuclide transport

The horizontal fracture plane and the vertical fault plane intersect perpendicularly with each other at the center of the cubic domain. The leak boundary is assumed in the intersection region between the repository and the horizontal fracture. A constant solute concentration is located in the leakage region. Table 2 shows the numerical parameters of nuclide migration.

Figure 3 (a) shows the evolution of the aperture and flow velocity. The aperture and flow velocity reduce remarkably at 10^2 years due to the thermal expansion around the repository. Then, the aperture gradually recovered and the flow velocity increased as the in-situ stress and heat disappeared. Figure 3 (b) shows the typical concentration contour along the horizontal and vertical fractures at 10^4 years. The nuclide transports from the repository to the ground surface with fluid flow along the fractures. Figure 4 shows the nuclide transport with and without thermal effect. The thermal conductivity is equal to 0, which means that there is no thermal effect. The observed delayed transport with thermal effect is due to the aperture closure and the slow flow caused by the thermal expansion around the repository.

The influence of thermal conductivity on nuclide transport was investigated since it is the most important material parameter (Hudson et al. 2005). The thermal conductivity of backfilled materials in repositories could be vary by as much as an order of magnitude (Rutqvist 2020). Hence, the varies thermal conductivities of the repository are discussed incorporated into the model to understand the nuclide transport behavior. Figure 4 shows the nuclide transport on the horizontal fracture plane with three thermal conductivities. The higher thermal conductivity in the repository induces to faster thermal decay and ultimately facilitates the nuclide transport.

Table 2. Numerical parameters for nuclide migration in a 3D nuclear waste repository.

Property	Symbol	Unit	Material	Value
Fracture aperture	b_v	mm	Vertical fracture	5.0
	b_h		Horizontal fracture	1.0
Porosity	ϕ_f	-	Fracture	0.9
	ϕ_m		Matrix	0.01
Dispersity	α_x, α_y	m	Fracture	0.1
Molecular diffusion coefficient	D^*	m^2/s	Fracture	1.6e-9
Solute concentration	c_0	mol/m^3	Fracture	1

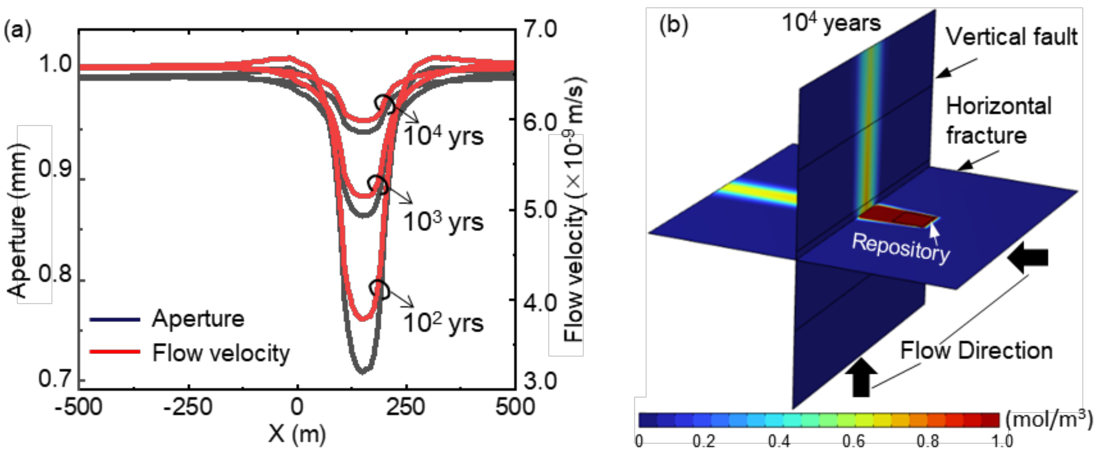

Figure 3. (a) Evolution of aperture and flow velocity. (b) Concentrations at the horizontal and vertical fractures of 10^4 years.

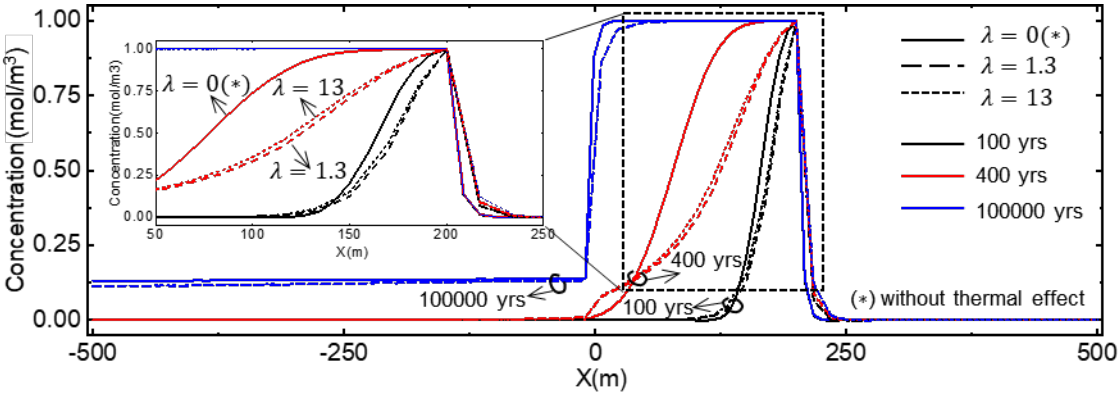

Figure 4. Concentrations at the horizontal fractures. The enlarged view shows the concentration under different thermal conductivities and without thermal effect.

4 CONCLUSIONS

The thermal effect was highlighted and a 3D repository model was developed to understand the nuclide transport behavior. The thermal expansion induces the aperture closure and the slow flow around the repository, which finally retards the nuclide transport. The higher thermal conductivity in the repository induces to faster thermal decay and ultimately facilitates the nuclide transport.

ACKNOWLEDGEMENT

This work is supported by the National Natural Science Foundation of China (U2067203, 42277140).

REFERENCES

Chang KW, LaForce T, Price LL. 2022. Hydro-thermal impacts on near-field flow and transport in a shale-hosted nuclear waste repository. *Tunnelling and Underground Space Technology* 130, pp. 104765. DOI: 10.1016/j.tust.2022.104765

Guo R, Xu H, Plúa C, Armand G. 2020. Prediction of the thermal-hydraulic-mechanical response of a geological repository at large scale and sensitivity analyses. *International Journal of Rock Mechanics and Mining Sciences* 136, pp. 104484. DOI: 10.1016/j.ijrmms.2020.104484

Hudson JA, Stephansson O, Andersson J. 2005. Guidance on numerical modelling of thermo-hydro-mechanical coupled processes for performance assessment of radioactive waste repositories. International *Journal of Rock Mechanics and Mining Sciences* 42, pp. 850–870. DOI: 10.1016/j.ijrmms.2005.03.018

Min KB, Rutqvist J, Tsang CF, Jing L. 2005. Thermally induced mechanical and permeability changes around a nuclear waste repository - A far-field study based on equivalent properties determined by a discrete approach. *International Journal of Rock Mechanics and Mining Sciences* 42, pp. 765–780. DOI: 10.1016/j.ijrmms.2005.03.014

Rutqvist J. 2020. Thermal management associated with geologic disposal of large spent nuclear fuel canisters in tunnels with thermally engineered backfill. *Tunnelling and Underground Space Technology* 102, pp. 103454. DOI: 10.1016/j.tust.2020.103454

Tang DH, Frind EO, Sudicky EA. 1981. Contaminant transport in fractured porous media: Analytical solution for a single fracture. *Water Resources Research* 17, pp. 555–564. DOI: 10.1029/WR017i003p00555

Tsang C-F, Neretnieks I, Tsang Y. 2015. Hydrologic issues associated with nuclear waste repositories. *Water Resources Research* 51, pp. 6923–6972. DOI: 10.1002/2015WR017641